International Journal of Modern Physics C, Vol. 11, No. 5 (2000) 1–12

SYSTEM FOR AUTOMATIC DETECTION OF CLUSTERED MICROCALCIFICATIONS IN DIGITAL MAMMOGRAMS

A. BAZZANI, D. BOLLINI, R. BRANCACCIO, R. CAMPANINI,
N. LANCONELLI, and D. ROMANI

Department of Physics, University of Bologna and National Institute for Nuclear Physics, viale Berti Pichat, 6/2, 40127 Bologna, Italy

A. BEVILACQUA

Department of Electronics, Computer Science and Systems University of Bologna, viale Risorgimento 2, 40136 Bologna, Italy

National Institute for Nuclear Physics viale Berti Pichat, 6/2, 40127 Bologna, Italy
E-mail: *bevila@bo.infn.it*

Received 9 June 2000
Revised 4 July 2000

In this paper, we investigate the performance of a Computer Aided Diagnosis (CAD) system for the detection of clustered microcalcifications in mammograms. Our detection algorithm consists of the combination of two different methods. The first, based on difference-image techniques and gaussianity statistical tests, finds out the most obvious signals. The second, is able to discover more subtle microcalcifications by exploiting a multiresolution analysis by means of the wavelet transform. We can separately tune the two methods, so that each one of them is able to detect signals with similar features. By combining signals coming out from the two parts through a logical OR operation, we can discover microcalcifications with different characteristics. Our algorithm yields a sensitivity of 91.4% with 0.4 false positive cluster per image on the 40 images of the Nijmegen database.

Keywords: Computer Aided Diagnosis; Digital Mammograms; Image Processing; Microcalcifications; Wavelet; Pattern Recognition; CAD.

1. Introduction

Breast cancer is the most common form of cancer among women. The presence of microcalcifications in breast tissues is one of the main features considered by radiologists for its diagnosis. Unfortunately, according to statistical results, the error in microcalcifications detection is relevant for population screening programmes. One of the possible solutions to reduce detection errors could be to assist doctors with a computer-aided system. The computer output is presented to radiologists as a "second opinion" and can improve the accuracy in the detection task.[1]

Several techniques developed for the automated detection of microcalcifications can mainly be grouped in three different categories: Multiresolution analyses, filtering methods and statistical methods. Multiresolution analyses,[2–4] based on wavelet transform of mammograms, magnify the typical microcalcifications scales. Filtering methods remove the structured background in order to isolate microcalcifications-like signals.[5] Statistical methods are based on Bayesan decision techniques[6] or gaussianity tests with an adaptive filtering.[7]

By comparing the different methods, it turns out that some microcalcifications are detected by one method but missed by the others.

In this paper, we propose an approach based on the combination of different detection methods in order to get optimal performances: The simultaneous use of two or more techniques might improve the results of an optimized single method.[8]

The basic idea of our method is to combine a multiresolution analysis based on wavelet transform with a difference-image method and a gaussianity statistical test and to perform a logical OR operation on the detected microcalcifications before clustering.

In the difference-image part of the algorithm, we pre-process an image by an adaptive noise equalization[6] and we choose the Regions Of Interest (ROI's) by means of a gaussianity test. Gray-level local thresholding is then employed, followed by a false-positive reduction task based on local edge-gradient analyses.

In the wavelet section, we study ROI's by using both a multiresolution analysis and a high local contrast filter: In this way, we select signals having small size and high local contrast. Multiresolution is performed by means of wavelet transform. A hard thresholding is applied to the coefficients of the smallest scale and the ROI's are reconstructed by using the coefficients of the first three scales. Then, a gray-level local thresholding is realized. False positive signals are eliminated by means of morphological operators and local edge-gradient analyses.

Finally, we clusterize the microcalcifications by performing the logical OR operation on signals detected by the two methods.

The performance of detection scheme has been tested on 40 digitized mammograms coming from Nijmegen Hospital: This database is considered as a benchmark for Computer Aided Diagnosis (CAD) systems. The total number of clusters is 105 and there are considerable variations of visibility among them. The images have been digitized to a pixel size of 0.1×0.1 mm^2 and quantizied to 12-bits gray scales.

Recent studies[9] have shown that CAD techniques originally developed on digitized mammograms may be applied to analyze full-field digital mammograms. The detection parameters could be modified, due to the properties of digital detector.

2. Methods

2.1. *Detection scheme*

Microcalcifications are very small spots which appear brighter than the surrounding normal tissue. Typically, they are between 0.1 mm and 1 mm in size and are of

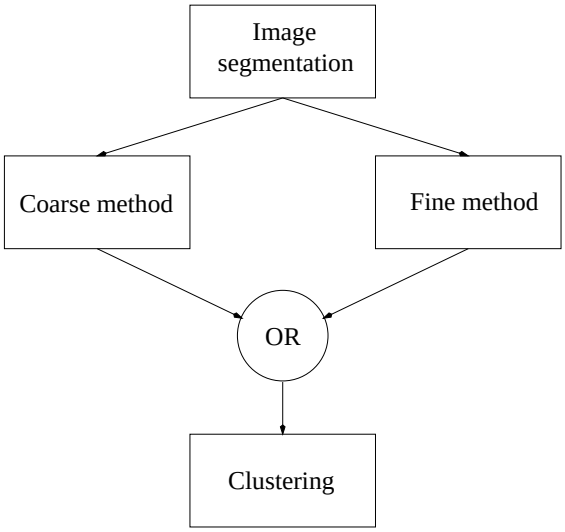

Fig. 1. Detection scheme.

particular clinical significance when found in clusters of five or more in a 1 cm^2 area. Most of the clusters consist of at least one evident microcalcification and other more hidden signals. In the Nijmegen database, the diameter size of clusters ranges from 2 mm to 50 mm.

Our approach includes two different methods: The first one (coarse) is able to detect the most obvious signals and uses difference-image techniques and gaussianity tests, while the second one (fine), based on multiresolution analyses, discovers more subtle microcalcifications.

The detection scheme of the algorithm is shown in Fig. 1. First, the digitized image is segmented to isolate breast tissues from image background. In this way, we reduce both the processing time and memory requirements, since we analyze only areas which contain useful information for the detection. The segmented image is then passed to the two signal-extraction methods described in the following subsections. Signals coming out from these methods are combined through a logical OR operation and then clusterized to give the final result.

2.2. *Coarse method*

In this part of the algorithm, we remove structured image background by means of a difference-image technique. The scheme of the coarse method is shown in Fig. 2. First of all, we perform an iso-precision noise equalization.[6] In this way, we optimize the choice of gray-level thresholding parameter k as shown in Fig. 2.

The equalized image is passed through two different filters: A 3×3 match-filter that produces a signal-enhanced image and a 7×7 box-rim filter that gives a signal-suppressed image.

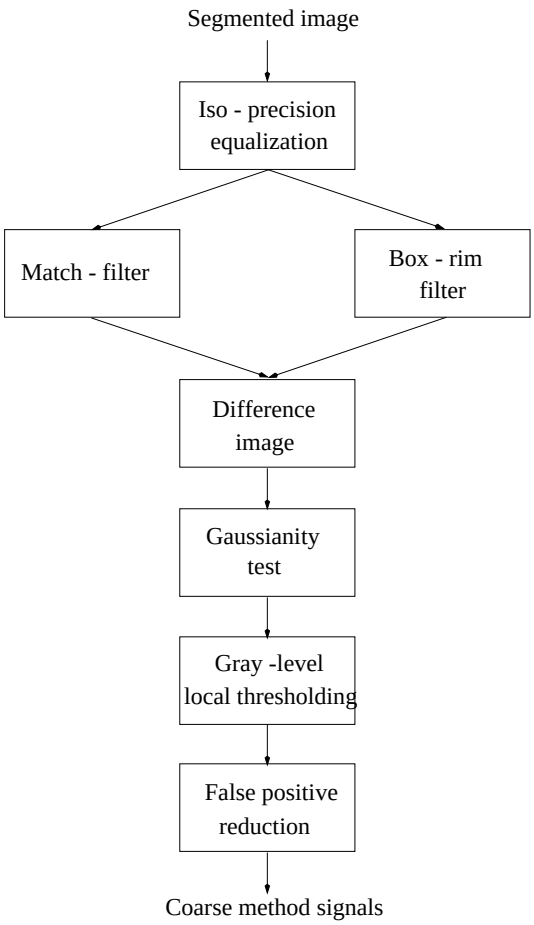

Fig. 2. Scheme of the coarse method.

The match-filter approximates the mean contrast variations of a typical microcalcification and enhances signals having similar size and local contrast. The box-rim filter suppresses high-frequency noise maintaining the low-frequency structured background. The box-rim filter averages all the $n \times n$ neighbor pixels except those inside a kernel in the middle of the window filter: We use a 7×7 window with a 3×3 null kernel inside.

By subtracting the suppressed image from the enhanced one, we obtain a difference-image, which contains noise and signals resembling microcalcifications. According to experimental evidences, we assume that the remaining noise is gaussian, since we have reduced the structured noise in the previous steps. We then employ a gaussianity test on the difference image in order to choose ROI's that include interesting signals. This test is based on the first three moments I_1, I_2, and ${I_3}^7$ of the gray-level distribution in a 51×51 pixels window in difference image. For

a gaussian distribution with mean μ and variance σ^2, the moments I_1, I_2 and I_3 converge to:

$$\begin{aligned} I_1 &\to \mu \\ I_2 &\to \sigma^2 + \mu^2 \\ I_3 &\to \mu^3 + 3\sigma^2\mu \end{aligned} \quad .$$

Consequently, we have: $h = I_3 - 3I_1(I_2 - I_1^2) - I_1^3 = 0$.

Since the difference-image contains only gaussian noise and signals with a high contrast, we should have a deviation from gaussianity in regions including microcalcifications, hence, a high value of h is supposed to appear in these zones. We measure h in 80 windows containing microcalcifications and in 80 windows without them. In Fig. 3, distributions of h values are depicted. We fix a threshold in order to find out "suspect" ROI's and then we perform the gray-level thresholding only in ROI's having value of h greater than the threshold. With a threshold equal to $h_t = 0.9$, we reject 80% of the considered ROI's losing only 2% of ROI's containing microcalcifications.

The central pixel of the considered 51×51 window of the difference-image is retained only if its gray level is greater than $\mu + k\sigma$, where k is the parameter which gives the variation on the coarse method sensitivity. Connected pixels are then grouped into a single signal.[10]

The next step is a false-positive reduction (fpr) phase based on a local edge-gradient analysis.[11] We consider five features (*area*, *average pixel value*, *edge*

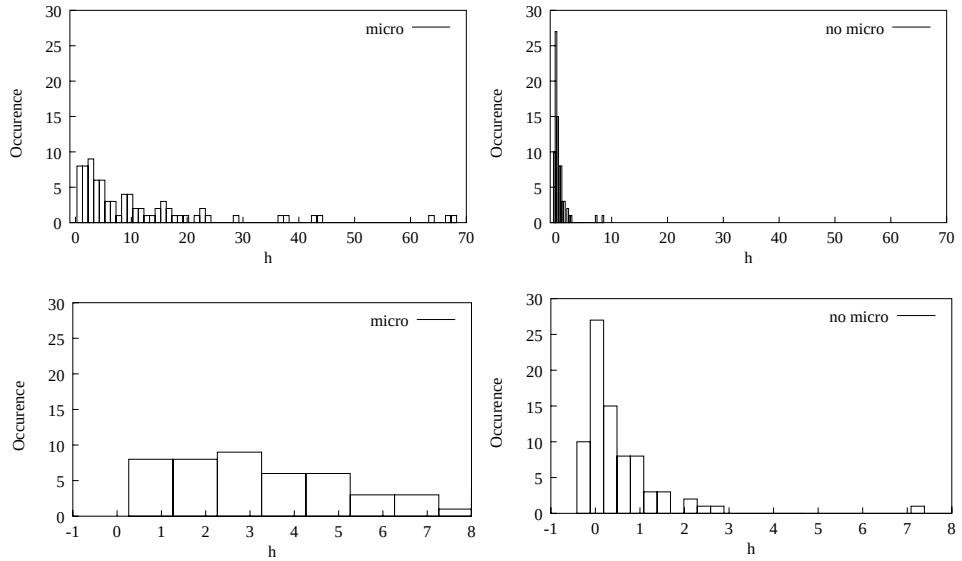

Fig. 3. Top: Complete histograms. Bottom: Zoom of the histograms in the zone where threshold is applied ($h_t = 0.9$). Left: Histogram of h values in windows containing microcalcifications. Right: Histogram of h values in windows without microcalcifications.

gradient, *degree of linearity*, *and average local gradient*) to separate microcalcifications from false signals.

In the Nijmegen database, we select signals having an *area* ranging from a couple of pixels to some dozen of pixels. Features such as *average pixel value* and *edge-gradient* help to remove signals that look like subtle or blurred microcalcifications and signals due to artifacts. By using a linear pattern analysis (*degree of linearity* and *average local gradient*), we eliminate signals caused by bright linear patterns. Signals surviving the fpr stage will combine with others coming from the fine method described in the next subsection.

2.3. *Fine method*

In this part of the detection scheme, we try to discover more subtle microcalcifications by means of multiresolution analyses based on the wavelet transform. Figure 4 depicted the scheme of the fine algorithm.

Microcalcifications are characterized by well-defined range size and high local contrast, so, we find out signals having these features. We split the algorithm into two independent sections. The first one detects signals having size smaller than 1 mm by means of a multiresolution analysis. In the second section, signals having a high local contrast are enhanced by using a difference image technique. We then perform an AND logical operation in order to find out signals having both the

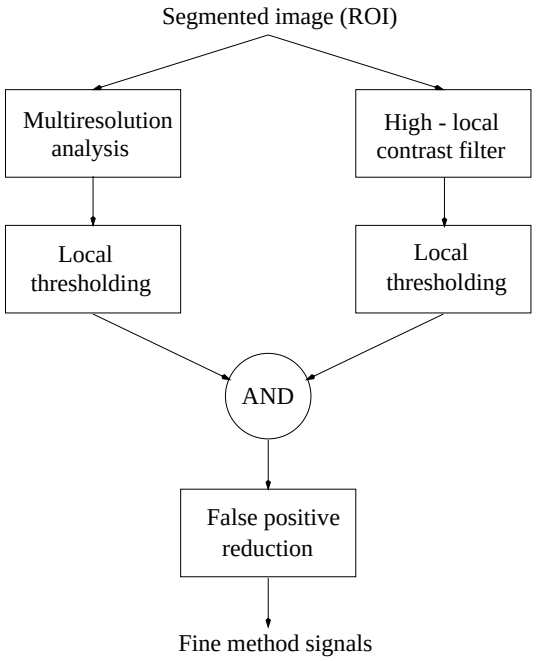

Fig. 4. Scheme of the fine method.

features we are looking for. The AND operation is necessary to eliminate spurious signals introduced by multiresolution analysis due to the nonuniform structure of breast tissue.

The scheme of multiresolution analysis is shown in Fig. 5. We want to stress that we perform a hard thresholding on scale 1^{12}: To reconstruct the image, we maintain only coefficients having value greater than 1.5σ (with σ standard deviation of the coefficients distribution). Scale 1 includes both high-frequency noise and useful information about microcalcifications; by using the hard thresholding, we try to reduce noise effects and, at the same time, to keep information about microcalcifications. We utilize a Least Asymmetric Daubechies' (LAD8) mother wavelet for the multiresolution analysis. To extract interesting signals, we perform a local thresholding in 40×40 pixel size windows. Assuming a gaussian distribution for the noise, we fit with a parabola the gray level histogram of the window in semilogarithmic scale (Fig. 6). Then, we retain pixels having a gray level greater than the intersection of parabola with x axis. In order to eliminate spurious signals, we accomplish a morphological opening operation on the image.

The second section of fine method is based on a difference-image technique similar to the one described in coarse method. We subtract a suppressed image obtained by a 9×9 moving average filter from an enhanced image coming from a 3×3 match-filter. We carry out the same local thresholding on the difference image followed by the morphological opening. In Fig. 6, we show the histogram of windows of the difference image where the gray level local thresholding is performed. After

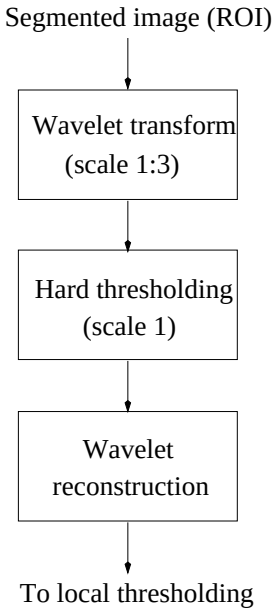

Fig. 5. Scheme of the multiresolution analysis.

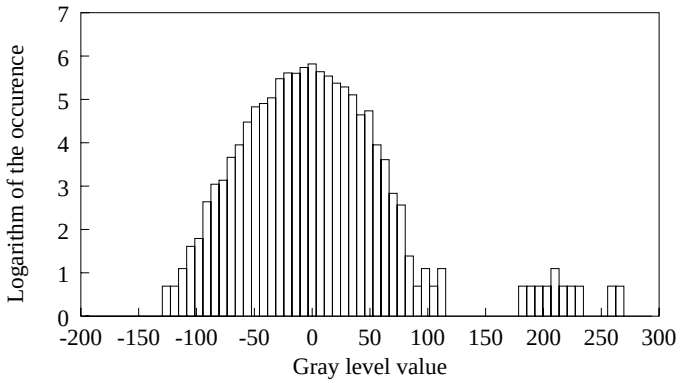

(a)

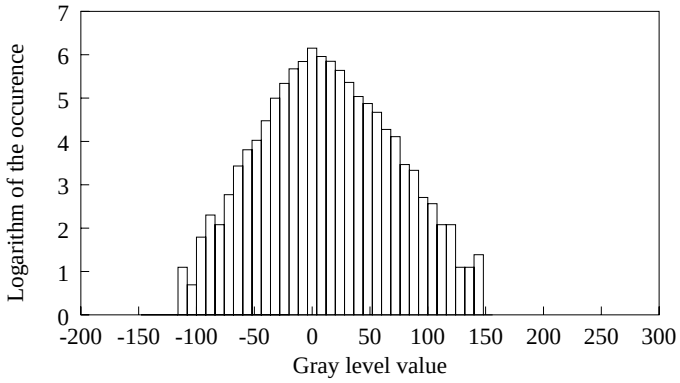

(b)

Fig. 6. Histogram of windows of the difference image where gray level local thresholding is performed. (a) Window containing microcalcifications, (b) Window without interesting signals.

that, a logical AND operation is accomplished on signals extracted by the two sections of fine method.

To split false signals from microcalcifications, a fpr phase similar to the one seen in coarse method is performed. In Fig. 7, we show the distribution of two fpr features (*edge gradient vesus gray level*) and the chosen curve which separates false signals from microcalcifications; this curve f has the form: $f(x) = p_1 \tanh(p_2 x)$. Features values are calculated on the original digitized image. Finally, microcalcifications which have passed the fpr step are combined with others coming from coarse method through a logical OR operator.

2.4. *Clustering*

There are different definitions of clusters and several strategies in the estimation of true positive and false positive rates.[13] We define cluster an ensemble of three or

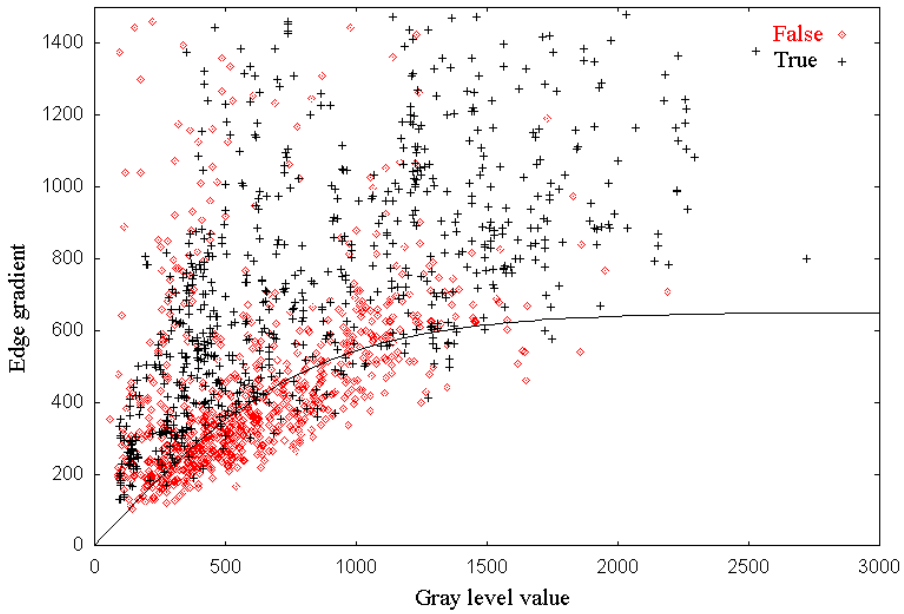

Fig. 7. Distribution of *edge gradient versus gray level* for true (plus signs) and false (diamonds) signals.

more signals having each one at least another signal in a 5 mm neighbor. Following this statement, we clusterize all microcalcifications coming from the OR operation and calculate center and radius of each cluster. The center of cluster is computed as the centroid of signals belonging to it, while its radius is the maximum distance between signals and the center of cluster. In order to classify a cluster as true or false, we adopt the following criterion: A cluster is defined true if its center falls inside the suspect area marked by radiologists.

3. Results

The goal of this paper is to show the combination of different methods allows the detection of microcalcifications that could have been missed by using one detection technique alone. In Fig. 8, we can see an example which explains this fact. A cluster containing eight microcalcifications is depicted (labeled from 1 to 8). The most obvious signals (3, 4, and 6) are detected by both methods. These signals have high *local contrast* and high Signal to Noise Ratio (*SNR*). We consider as noise every structure of the image having a size greater than some dozen of pixels (maximum microcalcifications area). It is important to note that with the term *local contrast* we mean a contrast computed on a small neighbor (a couple of pixels). We estimate *SNR* as the ratio between the signal gray-level and the average gray-level computed in a neighbor of 50×50 pixels. We are searching for signals having small size and high *local contrast*.

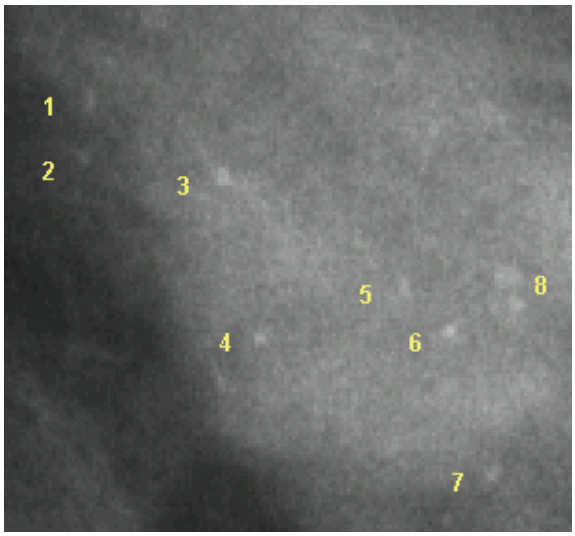

Fig. 8. Cluster containing eight microcalcifications.

In the example depicted in Fig. 8, we can see that the fine method can discover signals with low *SNR*, while the coarse method misses them: The reason is that the wavelet transform can enhance in better way signals similar in size to microcalcifications. Microcalcifications 1, 2, and 5 are detected by the coarse method but missed by the fine one. They are characterized by high *SNR* and low *local contrast*. The fine method is not able to find out them because their *local contrast* is not very high and they are confused with spurious signals which have the same size of the microcalcifications. Signals 7 and 8 are discovered by the fine method but missed by the coarse one because they have a low *SNR* (i.e., these signals are characterized by a high *local contrast*, but at the same time they are surrounded by bright structured background). In this example, the simultaneous use of the two methods permit the detection of all microcalcifications of the cluster. An example of the performance of our detection algorithm is shown in Fig. 9 for some sets of parameters. Three Free Response Operating Characteristics (FROC) curves are depicted: One related to the combined method, one for the coarse method and one for the fine one. The curves are obtained by varying the following parameters: k in the coarse and in the combined method curves, p_1 and p_2 in the fine one. There is a clear improvement due to the simultaneous use of the two methods. We have at least a sensitivity over 90% with a false positive alarm under 0.5 false per image (actually 91.4% with 0.4 false per image). These results are comparable to others obtained with the same database.[6,14–16]

The development of a CAD system consists of two steps. The first one concerns with parameters optimization: In order to test different sets of parameters, several hundreds of interactive runs on the whole database are needed. Each run takes

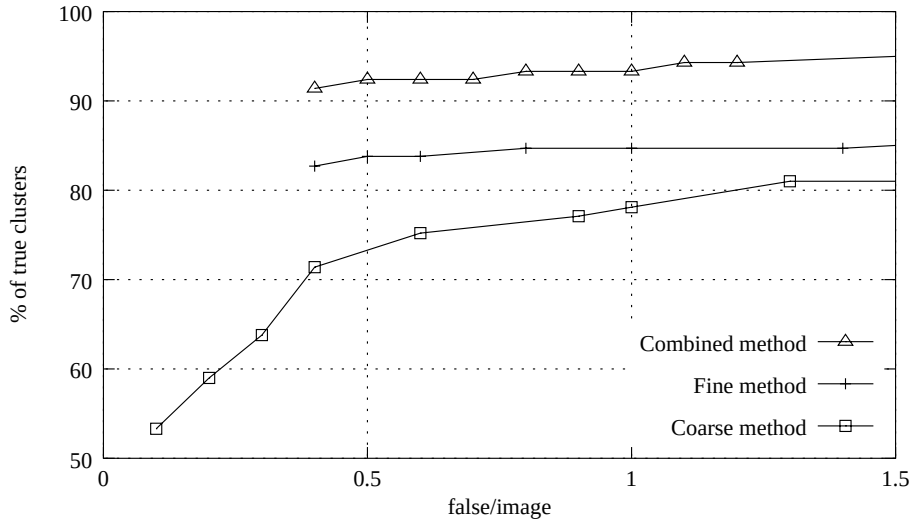

Fig. 9. FROC of our detection system on the Nijmegen database.

about 80 minutes (elapsed time), with no relevant external load, and 20 MB RAM. The second phase takes place when parameters have been tuned: The system is ready for the detection on a new image. The analysis of one single image requires small computational resources: About 20 MB RAM and 2 min (elapsed time). The computer used is an entry-level PC mounting a Pentium II 400 MHz processor. The code has been developed by using the C language and no-cost, free-source software: An X-based GUI, the gcc compiler and Linux OS.

4. Conclusion

In this paper, we have investigated the combination of different methods in the detection of clustered microcalcifications in digital mammograms. The first method is based on difference-image techniques and statistical tests while the second one employs a multiresolution analysis of the digital image. In this way, we can tune each part of the detection scheme so that each method is able to discover microcalcifications with similar features. By combining signals detected through a logical OR operation, we can therefore find out signals with different characteristics.

Results using the Nijmegen database have shown that our approach can lead to good performances.

Acknowledgments

Images were provided by courtesy of the National Expert and Training Center for Breast Cancer Screening and the Department of Radiology at the University of Nijmegen, the Netherlands.

This work is supported by Italian National Institute for Nuclear Physics (CALMA project).

Authors would like to thank Prof. F.-L. Navarria for his interest in the present work.

References

1. H. P. Chan, K. Doi, R. A. Schmidt, C. E. Metz, K. L. Lam, T. Ogura, Y. Wu, C. J. Vyborny, and H. MacMahon, *Invest. Radiol.* **25**, 1102 (1990).
2. H. Yoshida, K. Doi, and R. M. Nishikawa, *Proc. SPIE* **2167**, 868 (1994).
3. W. Zhang, H. Yoshida, R. M. Nishikawa, and K. Doi, *Med. Phys.* **25**, 949 (1998).
4. M. J. Lado, P. G. Tahoces, A. J. Mendez, M. Souto, and J. J. Vidal, *Med. Phys.* **26**, 1294 (1999).
5. H. P. Chan, K. Doi, S. Galhotra, C. J. Vyborny, H. MacMahon, and P. M. Jokich, *Med. Phys.* **14**, 538 (1987).
6. N. Karssemeijer, *IJPRAI* **7**, 1357 (1993).
7. M. N. Gurcan, Y. Yardimci, and A. E. Cetin, *Digital Mammography* (Kluwer Academic Pub., Nijmegen, 1998), p. 157.
8. H. Yoshida, K. Doi, R. M. Nishikawa, M. L. Giger, and R. A. Schmidt, *Acad. Radiol.* **3**, 621 (1996).
9. L. M. Yarusso, R. M. Nishikawa, M. L. Giger, J. Papaioannou, A. E. Baehr, L. A. Venta, R. Nagel, and M. A. Kupinski, to appear on *Proeedings of IWDM 2000* (Med. Phys. Pub., Madison, WI, USA, 2000).
10. R. M. Nishikawa, M. L. Giger, K. Doi, C. J. Vyborny, and R. A. Schmidt, *Med. Phys.* **20**, 1661 (1993).
11. T. Ema, K. Doi, R. M. Nishikawa, Y. Jiang, and J. Papaioannou, *Med. Phys.* **22**, 161 (1995).
12. D. L. Donoho and I. M. Johnstone, *J. Amer. Statist. Assoc.* **90**, 1200 (1995).
13. M. Kallergy, G. M. Carney, and J. Gaviria, *Med. Phys.* **26**, 267 (1999).
14. W. Veldkamp and N. Karssemeijer, *Digital Mammography* (Kluwer Academic Pub., Nijmegen, 1998), p. 169.
15. S. Brown, R. Li, L. Brandt, L. Wilson, G. Kossof, and M. Kossof, *Digital Mammography* (Kluwer Academic Pub., Nijmegen, 1998), p. 189.
16. J. M. Mossi and A. Albiol, *Digital Mammography* (Kluwer Academic Pub., Nijmegen, 1998), p. 475.